Structure-based Design of CBP/EP300 Degraders: When Cooperativity Overcomes Affinity

Iván Cheng-Sánchez,[a, ‡] Katherine Gosselé,[a,b, ‡] Leonardo Palaferri,[a, ‡] Eleen Laul,[a] Gionata Riccabella,[a] Rajiv K. Bedi,[b] Yaozong Li, [b] Anna Müller, [b] Amedeo Caflisch[b,*] and Cristina Nevado[a,*]

a Department of Chemistry, University of Zurich, Winterthurerstrasse 190, CH-8057 Zurich, Switzerland

b Department of Biochemistry, University of Zurich, Winterthurerstrasse 190, CH-8057, Zurich, Switzerland

‡ These authors contributed equally

ABSTRACT: Here we present the development of **dCE-2**, a structurally novel PROTAC targeting the CREB-binding protein (CBP) and E1A-associated protein (EP300) – two homologous multidomain enzymes crucial for enhancer-mediated transcription. The design of **dCE-2** was based on the crystal structure of an in-house bromodomain (BRD) inhibitor featuring as acetyl-lysine mimic a 3-methyl cinnoline discovered by high-throughput fragment docking. Our study shows that, despite its modest binding affinity to CBP/EP300-BRD, **dCE-2** remarkable protein degradation activity stems from its excellent cooperativity, which we demonstrate by the characterisation of its ternary complex formation both *in vitro* and *in cellulo*. Molecular dynamics simulations indicate that in aqueous solvent this active degrader populates both folded and extended conformations which are likely to promote cell permeability and ternary complex formation, respectively.

KEYWORDS: PROTAC, Fragment docking, Cooperativity, Structure-based design, Chameleon effect, CBP, EP300, Bromodomain

INTRODUCTION

Proteolysis targeting chimeras (PROTACs) are an emerging class of small molecules that induce target protein degradation by hijacking the cellular proteolysis machinery. Structurally, PROTACs are heterobifunctional molecules that consist of a ligand for the target protein of interest (POI) connected via a linker to a ligand for an E3 ubiquitin ligase. PROTACs initiate a degradation process by establishing a ternary complex involving the POI and the E3 ligase, which end up in close proximity and result in the polyubiquitination and subsequent proteasomal degradation of the POI.[1–4] Unlike classical small molecule drugs that rely on an occupancy-driven mechanism, PROTACs achieve complete loss of function of the target protein following a brief binding event. In addition, PROTACs can operate in a catalytic fashion and enhance specificity for close homologues through additional protein-protein interactions (PPIs) between the POI and the E3 ligase.[5–7]

Despite their advantages, PROTACs are significantly larger than the POI ligands from which they derive and generally suffer from poor pharmacokinetic profiles and low cell permeability.[8–10] To address these problems, recent efforts have been devoted to understanding the physicochemical properties and structure-property relationships of PROTACs.[11–17] Besides classical parameters, the ability to quickly form a ternary complex stabilised by protein-protein interactions (PPIs) plays a crucial role in PROTAC-mediated degradation which, together with their catalytic mechanism can compensate for some of the abovementioned issues.[8] The different binding affinities of PROTACs to each target protein in the presence of the other is referred to as cooperativity (α) and corresponds to the ratio between the degrader's binary and ternary affinity. Individually measuring binary ligand affinity during an early PROTAC screening can generate valuable information on structure-activity relationships (SAR) but does not account for the influence of PPIs on ternary complex stability. Therefore, rational analysis to understand PPIs is essential in PROTAC development, but it generally requires obtaining ternary complex crystal or cryo-EM structures, which is far from being a routine task.[18–23] In consequence, PROTAC development relies heavily on large empirical dataset of synthesized compounds so that methods to better understand the correlation between the physicochemical properties of PROTACs and their target degradation ability are on high demand.

Herein, we present the protein structure-based development of a novel degrader, **dCE-2**, targeting CREB-binding protein (CBP) and E1A-associated protein (EP300). CBP and EP300 are two transcriptional cofactors that regulate gene expression[24-26] through numerous PPIs[27] and by acetylating histone and non-

histone proteins.[28,29] CBP/EP300 are implicated in a wide range of diseases, such as cancer, inflammation and developmental disorders.[30–34] Five CBP/EP300 PROTACs based on different bromodomain (BRD)[35–37] and histone acetyl transferase (HAT)[38,39] ligands have been reported by our[40] and other groups. [41–44] In this work, we used high throughput docking[45] to identify an unprecedented 3-methyl cinnoline fragment as acetyl-lysine mimic. Subsequent structure-based optimization of this fragment led to the discovery of a bromodomain (BRD) inhibitor,[46] which was further developed into PROTAC **dCE-2**. In depth characterisation of our degrader showed that, despite its modest binding affinity to CBP/EP300-BRD, it induces robust ternary complex formation with excellent cooperativity, both *in vitro* and *in cellulo*. Explicit water molecular dynamics (MD) simulations suggest that **dCE-2** is able to populate both folded and extended conformations which are likely to promote cell permeability and ternary complex formation respectively, thus signalizing the need for a broader set of parameters to streamline the design of efficient PROTACs.

HIGH-THROUGHPUT FRAGMENT DOCKING AND WARHEAD SELECTION

At the beginning of this study, we decided to identify a potent and selective fragment hit using docking into the bottom of the acetyl-lysine pocket. The docking program SEED[47] was employed as it is very efficient (about 2s per fragment, see Supporting Information) and has produced hit fragments for a large variety of protein targets of pharmaceutical relevance.[48–54] The binding energy evaluation in the program SEED is based on the CHARMM force field and an implicit model of the solvent.[47, 55–57] From the in silico screening of a library of about 500 small molecules (mainly heteroaromatics with molecular weight (MW) below 300 g/mol),[58] a 3-methylcinnoline moiety emerged as the fragment with the most favourable SEED-predicted binding energy (-19.9 kcal/mol), favourably comparing to previously reported *N*,*N*-dimethylacetamide (-19.5 kcal/mol)[59] and acetophenone (-16.3 kcal/mol)[60] scaffolds. Additionally, the methylcinnoline fragment displayed selectivity for CBP over the *N*-terminal bromodomain of BRD4 (BRD4(1)), with the predicted binding energy for BRD4(1) being -16.5 kcal/mol. The fragment-growing strategy was inspired by the visual analysis of the overlap of the docked pose of 3-methylcinnoline in the CBP bromodomain and the crystal structure of the complex with a previously reported acetophenone-based ligand also developed in house (compound 16 of Ref. 45; PDB code 5NLK) which suggested the replacement of the acetophenone group with the 3-methylcinnoline to generate compound **1** (Figure 1A). Subsequent optimization for *in cellulo* and *in vivo* applications resulted in compound **2**.[46] To ease PROTAC development and linker attachment, the furane of **2** was replaced by a methyl group leading to compound **3**. Compound **3** showed very good binding affinity (K_D CBP/EP300 = 29/35 nM) and an even better ligand efficiency (LE CBP/EP300 = 0.35) when compared to **2**. Based on the crystal structure of **1** in complex with CBP BRD (PDB:6SQM) and assuming a similar binding mode, the acetamide of **3** was chosen as a prominent position for future conjugation with the linker moieties.

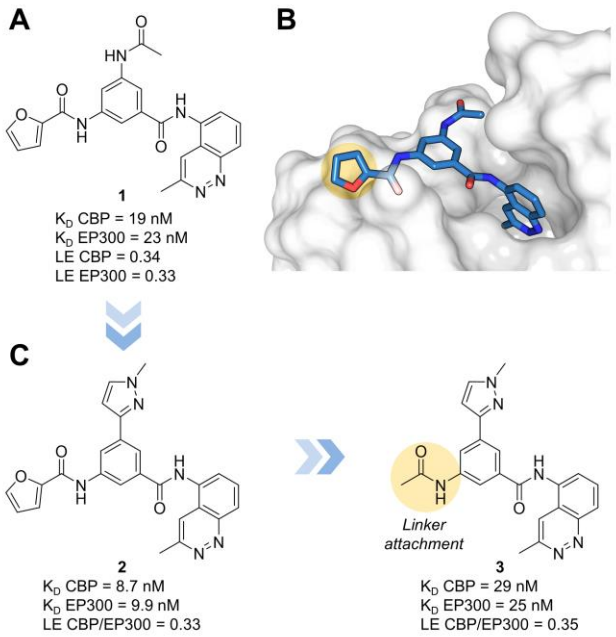

Figure 1. CBP/EP300-BRD ligands selected for structure-based optimization and PROTAC development. A) Chemical structure, CBP/EP300 K_D values and ligand efficiency (LE) of **1**. B) Crystal structure of **1** in complex with CBP bromodomain (PDB: 6SQM). C) Chemical structure, CBP/EP300 K_D values and LE of compounds **2** and **3**. Linker attachment site highlighted in yellow. K_D values were determined using BROMOscan™ technology.

PROTAC SYNTHESIS AND SCREENING

A small library[61] of potential degraders was prepared by conjugating various linkers at the acetamide vector site and targeting the Cereblon (CRBN) E3 ligase using thalidomide as ligand (Figure S1). To our pleasant surprise, compound **4** – featuring an 11-atom aliphatic linker – showed significant degradation of CBP, and to a lesser extent EP300, in the multiple myeloma LP1 cell line (5 μM compound, 16 h treatment). Next, linkers of different lengths and alternative points for the connection to the thalidomide ligand were explored resulting in compounds **4**-**9** (Figure 2). This small SAR campaign revealed the key role played by the linker length and the attachment point. Compared to our initial hit **4** (%remaining CBP/EP300 = 21/43), shortening the 11-carbon aliphatic linker by a single atom (**5**, **dCE-2**) slightly improved the degradation of CBP (% remaining = 16). However, further shortening the linker (8 carbon atoms, compound **6**) resulted in an abrupt loss of degradation (%remaining CBP/EP300 83/87), likely due to steric clashes between the two proteins. As **dCE-2** bears the most favourable linker length, we performed an optimization of the linker composition using this length. Conjugation via the 5' position to thalidomide (**7**) led to a slight decrease in degradation potency (%remaining CBP/EP300 = 30/69) while further attempts to improve solubility or cellular permeability through PEG (**8**, % remaining CBP/EP300 = 81/95) or piperazine groups (**9**, % remaining CBP/EP300 > 95) significantly reduced degradation. Thus, we selected **dCE-2** for in depth characterization.

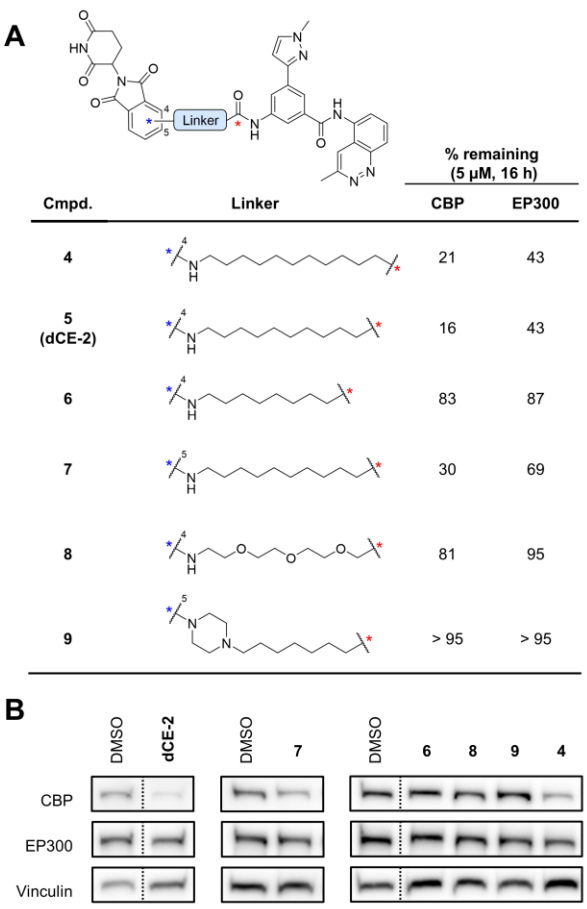

Figure 2. Refined PROTAC screen. A) Chemical structures of PROTAC molecules and quantification of CBP and levels by Western blotting following 16 hour treatment of LP1 cells with 5 μM compound. Vinculin was used as a loading control for normalization. B) Representative images of Western blots quantified in A), all images in Figure S2.

BIOLOGICAL CHARACTERISATION OF PROTAC dCE-2

To confirm that **dCE-2** induces CBP degradation through the expected PROTAC mechanism, we synthesized an analogue unable to bind CRBN by N-methylation of the thalidomide moiety (**10**, Figure 3A). As expected, this modification abrogated the degradation of CBP/EP300 (Figure 3B, left). Similarly, CBP degradation by **dCE-2** could be ameliorated through co-treatment with two structurally distinct CBP/EP300-BRD binders **2**[46] and GNE-781,[35] as well as with the CRBN ligand pomalidomide, confirming that degradation requires the engagement of both CBP-BRD and CRBN (Figure 3B, centre). Finally, CBP/EP300 degradation could also be blocked using the proteasome inhibitor MG132 (Figure 3B, right). **dCE-2** is a highly potent and efficient CBP PROTAC, able to reach a D_{max} >85 % with a DC_{50} of 40 nM in LP1 cells after 16 h (Figure 3C). CBP/EP300 degradation begins to occur within 2 h but requires 16-24 h to reach maximal degradation (Figure 3D). Further, **dCE-2** is an active degrader across a wide range of cancer cell lines including in an additional multiple myeloma cell line (MM1S), as well as the prostate cancer line LNCaP and the neuroblastoma line SH-SY5Y (Figure 3E). Interestingly, the bias for CBP degradation over EP300 was consistent across all cell lines.

dCE-2 displayed anti-proliferative effects in LP1 (GI_{50} = 1.513 μM) and MM1S (GI_{50} = 35 nM) cells at lower concentrations than both the parent inhibitor **2**, pomalidomide, and negative control **10** (Figure 3F), thus highlighting the advantage of protein degradation over simple inhibition. On the other hand, despite clear CBP degradation, **dCE-2** has little effect on the proliferation of LNCaP and SH-SY5Y cells, indicating that CBP and EP300 may not be essential for the growth of these lines (Figure S4).

CBP and EP300 were identified in global proteomics as two of the most downregulated proteins in both LP1 and MM1S cells following 16 h treatment with 1 μM **dCE-2** (Figure 3G and H), confirming their degradation in an antibody independent manner. Furthermore, MYC, a well-established downstream target of CBP and EP300, was also highly downregulated in both cell lines. In contrast, the expression of BRD4, a common off-target of CBP/EP300-BRD inhibitors, was not changed, confirming the specificity of **dCE-2** over other BRD containing proteins. In both lines the most strongly downregulated proteins were ZFP91 and IKZF1/3, all known substrates of immunomodulatory imide drugs (IMiDs).[62] Future work on modifying the CRBN binding moiety of **dCE-2** would be required to reduce the degradation of these proteins whilst maintaining the desired effects on CBP/EP300.

BINARY AFFINITY, TERNARY COMPLEX AND COOPERATIVITY

The binding affinity of **dCE-2** to the CBP- and EP300-BRDs was determined through a commercial service utilizing a ligand binding site-directed competition assay (BROMO*scan*™, Figure 4A). A significant loss of potency compared to the parent compound **3** (> 40-fold for CBP and > 400-fold for EP300) and a slight preference towards CBP binding was observed in these measurements. We subsequently determined the CBP-BRD IC_{50} using an in-house TR-FRET based competition assay, confirming the modest affinity of this PROTAC by another method (IC_{50} = 860 nM, Figure 4B). However, the binding of **dCE-2** was significantly improved in the presence of high concentrations of the CRBN C-terminal thalidomide binding domain (ternary IC_{50} = 108 nM, Figure 4B), demonstrating that formation of the CBP:**dCE-2**:CRBN ternary complex has good positive cooperativity (α = 8). We were also able to observe robust formation of the ternary complex using CBP-BRD and CRBN-thalidomide binding domain labelled with a TR-FRET pair. This assay afforded a classical hook curve with a good peak height at around 1 μM **dCE-2** (Figure 4C), which is consistent with a low affinity compound displaying positive cooperativity.[23] Together this biochemical data supports the ability of **dCE-2** to act as a PROTAC despite its modest (high nanomolar – low micromolar) affinity for CBP. It is apparent that **dCE-2** is an efficient PROTAC functioning through the expected mechanism, however its binary affinity to CBP is modest, especially in comparison to the parent small-molecule ligand **3**. To explore which factors may affect affinity, K_D values (BROMOscan, ™) were determined for all the PROTACs summarized in Figure 2A (Figure S5). This revealed that, despite having the same moiety for the bromodomain and the same moiety

for Cereblon, the K_D of these PROTACs is highly variable and very sensitive to subtle changes in the linker length and compo-

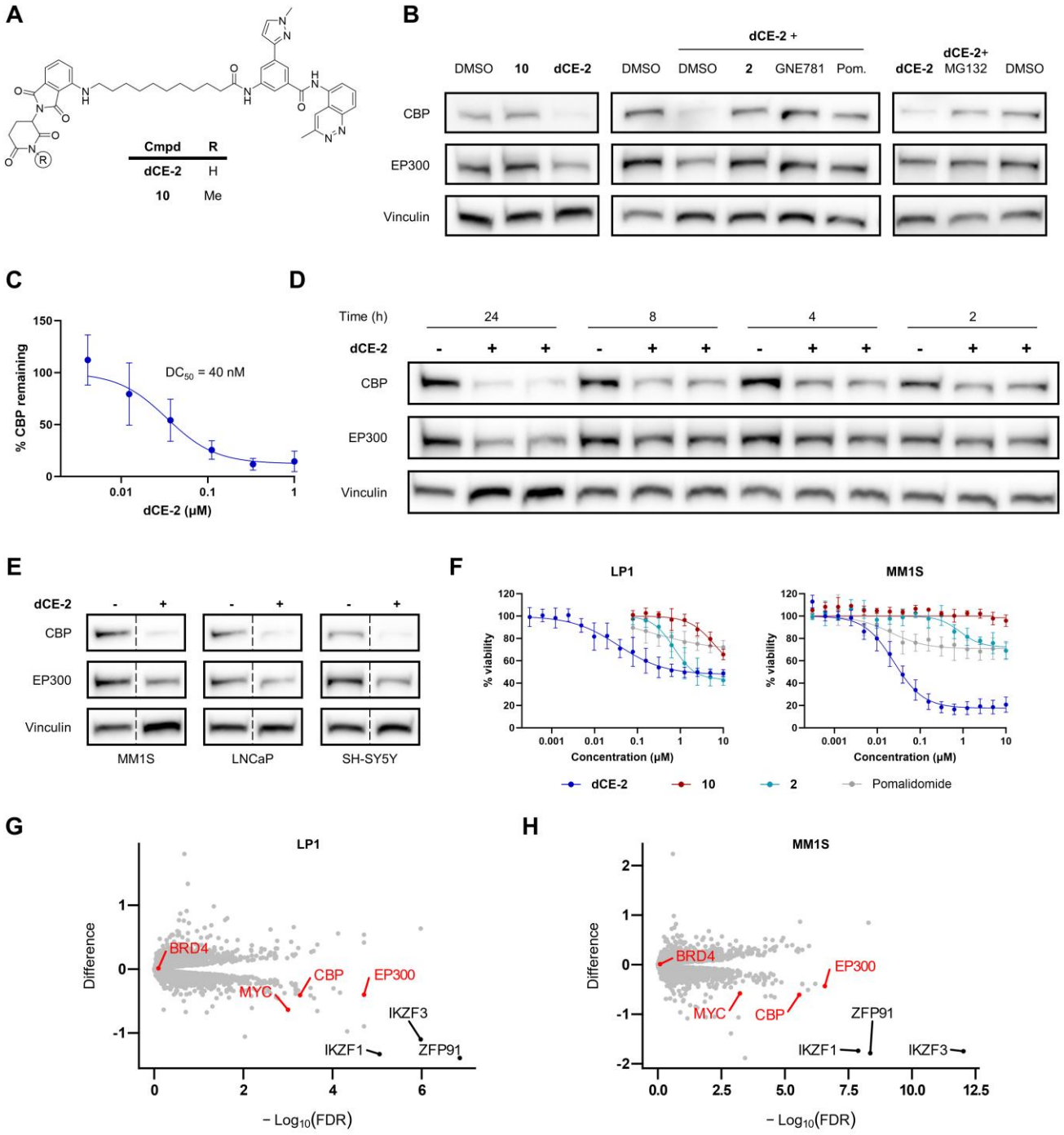

Figure 3. Characterization of **dCE-2**. A) Chemical structure of **dCE-2** and its negative control **10**. (B) Western blot measurements of CBP and EP300 levels in LP1 cells after 16 h with 1 μM **dCE-2** or the inactive analogue (left); pre-treated for 1 h with 10 μM **2** / 10 μM GNE-781 / 50 μM pomalidomide followed by 16 h 1 μM **dCE-2** (centre); pre-treated for 30 min with 10 μM MG132 (MG.) followed by 6 h 1 μM **dCE-2** (right). C) Dose response measurements of CBP levels by Western blot after 16 h treatment of LP1 cells with **dCE-2**. Western blot images used for quantification in Figure S3. D) Time course measurements of CBP and EP300 levels following treatment of LP1 cells with 1 μM **dCE-2**. E) Western blot measurements of CBP and EP300 levels in various cell lines following 16 h treatment with 1 μM **dCE-2**. F) LP1 and MM1s cell viability following 3-day compound treatment, determined using resazurin. Quantification of the global proteome of G) LP1 and H) MM1S cells following treatment for 16 h with 1 μM **dCE-2** compared to DMSO treated cells. Highlighted are the most significantly altered proteins (black, abs(difference) > 1 and -Log_{10}(FDR) > 5) and (in red) CBP, EP300, MYC and BRD4.

https://doi.org/10.26434/chemrxiv-2024-7w489 **ORCID:** https://orcid.org/0000-0002-3297-581X

sition. Interestingly an inverse correlation between the K_D and degradation ability was apparent (Figure S5).

We then turned our attention to the ability of these molecules to successfully form a ternary complex *in cellulo*. Thus, **dCE-2** and **4** – the two active degraders with modest (high nanomolar – low micromolar) affinity – were measured together with **9** which shows low nanomolar affinity but was unable to induce degradation of CBP/EP300 (Figure 4A) in a ternary complex formation assay using FluoPPI[63] (Fluorescent based technology detecting Protein-Protein Interaction). This method enables ternary complex formation to be observed in live cells through the formation of fluorescent foci. Despite their differences in affinity and ability to induce degradation, **dCE-2**, **4** and **9** were all able to induce good ternary complex formation in cells with CRBN and CBP-BRD (Figure 4D). Interestingly, the peak position of the hook curve, which is dependent upon a combination of the binary affinities for the CBP-BRD and CRBN,[23] occurs at a higher PROTAC concentration for **9**. Assuming that the CRBN affinity of **9** is not significantly worse than **dCE-2** and **4**, this suggests that the effective concentration of **9** is lower in cells, indicating relatively poor membrane permeability of this compound. Nevertheless, its hook curve is much wider, suggesting a better cooperativity of ternary complex formation.[23] Together, this data with the CBP-BRD cannot explain the difference in degradation ability of these compounds. In contrast, only the active degraders **dCE-2** and **4**, but not the inactive PROTAC **9**, are able to induce ternary complex formation with the CBP catalytic core (Figure 4D). This highlights that regions of the CBP protein beyond the BRD are involved in ternary complex formation, and thus suggests that the increased rigidity afforded by the piperazine group may hamper viable ternary complex formation in this case.

As the CBP-binding moiety is identical for these PROTACs, with the variations in linker occurring far from the bromodomain binding pocket, we hypothesized that the discrepancies in affinity could stem from differences in the intramolecular folding of the molecules. Furthermore, differences in folding would also contribute to cellular permeability by masking H-bond donors and acceptors and reducing the surface area of the molecule.[64] Thus, MD simulations were performed to map the conformations adopted by these PROTACs and their Solvent Accessible Surace Area (SASA) in aqueous environment. SASA correlates with extended (higher values) and compact (lower values) conformations of the molecule. Cluster analysis shows that **dCE-2** and **4** populate both compact and extended conformations, with 42 and 36% of the conformers having a SASA larger than 1300 Å^2, respectively. In contrast, compound **9**, predominantly populates extended conformations with 69% of the conformers having a SASA higher than 1300 Å^2. These differences can explain, at least in part, the less favourable K_D values of **dCE-2** as its compact folding in water may impair

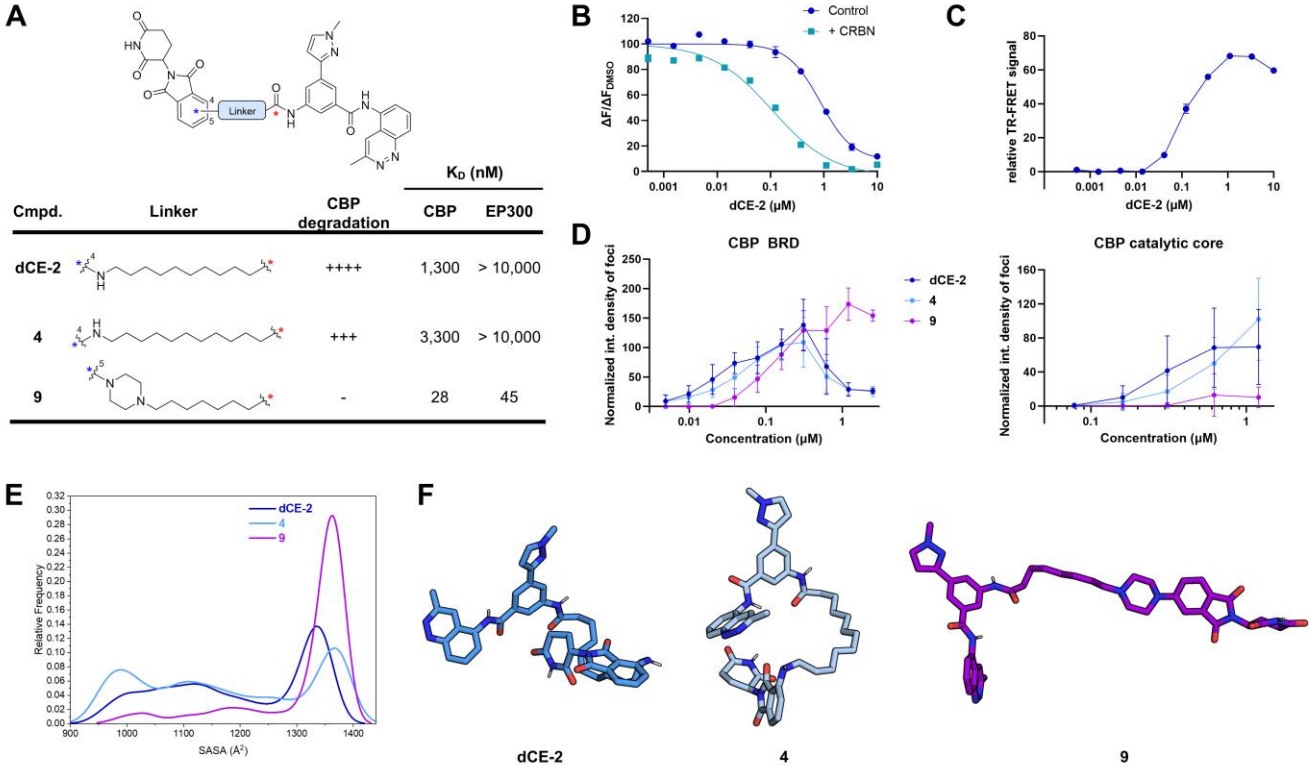

Figure 4. Mechanistic studies. A) Chemical structures, CBP degradation efficiency and binary affinities to CBP- and EP300-BRDs of selected compounds. K_D values were determined using BROMOscan™ technology. B**) dCE-2** binding to CBP-BRD in the presence and absence of high concentrations of CRBN, as determined through competition with acetylated peptide binding using TR-FRET. C) CBP-BRD: **dCE-2**:CRBN ternary complex formation as determined by TR-FRET. D) Cellular ternary complex formation as determined by the FluoPPI technology using the CBP-BRD or CBP catalytic core. Explicit water MD simulations of **dCE-2**, **4** and **9**: E) distribution of solvent accessible surface area (SASA) values along the 2.5 μs sampling of each PROTAC molecule, and F) representative conformer of the most populated cluster.

https://doi.org/10.26434/chemrxiv-2024-7w489 **ORCID:** https://orcid.org/0000-0002-3297-581X

binary binding in biochemical assays but aid its cell permeation. On the other hand, the flexible linker of **dCE-2** can allow population of extended conformations required for productive ternary complex formation. These results are in line with previous studies in which PROTACs with a chameleonic behaviour – *i.e.* the ability to mutate their conformation in environments with different polarity – showed improved aqueous solubility and cell permeability.[14]

CONCLUSIONS

In this work, we report the discovery and characterisation of a novel CBP/EP300 degrader **dCE-2**. This PROTAC is based on an in-house developed CBP/EP300 ligand, **3** (K_D CBP/EP300 = 29/25 nM). The development of the small-molecule ligand **3** was based on an unprecedented 3-methylcinnoline acetyl-lysine mimic identified by high-throughput docking, followed by fragment growing and subsequent optimization based on the crystal structure of a closely related analogue. Our protein structure-based analysis enabled the identification of a suitable attachment point within this ligand, which upon connection to a 10-atom aliphatic linker and a thalidomide CRBN E3 ligand resulted in **dCE-2**. Interestingly, this PROTAC is active across multiple cell lines (LP1, MM1S, LNCaP and SH-SY5Y) reaching its peak performance after 16 hours **(**DC_{50} = 40 nM). Furthermore, we show that **dCE-2** can form a ternary complex with CBP and CRBN both *in cellulo* (FluoPPI) and *in vitro* (TR-FRET) with high cooperativity (α = 8). Notably, MD simulations helped us rationalize why despite the modest K_D values of **dCE-2** toward CBP/EP300 bromodomains this PROTAC could degrade both proteins in a highly efficient manner: its ability to switch between a compact and an extended conformation might impair binding in biochemical assays but guarantee improved cell permeability. Thus, in contrast to small-molecule inhibitor development, binary affinity should not be the only parameter in early PROTAC screening. Collectively, our results led to the development of a novel CBP/EP300 PROTAC that further expands the toolbox of chemical probes to deconvolute the role of such proteins in disease development. Furthermore, by combining biological, biochemical, and computational techniques, we shed light on the correlation between binding affinity and degradation of structurally close degraders, thus highlighting that a multidisciplinary approach is essential to fully understand PROTAC SAR.

ASSOCIATED CONTENT

Supporting Information.
Methods, general procedures, experimental procedures and compound characterization (PDF). This material is available free of charge via the Internet at http://pubs.acs.org.

AUTHOR INFORMATION

Corresponding Author

* Cristina Nevado – Department of Chemistry, University of Zurich, Winterthurerstrasse 190, CH-8057 Zurich, Switzerland.
E-mail: cristina.nevado@chem.uzh.ch
* Amedeo Caflisch – Department of Biochemistry, University of Zurich, Winterthurerstrasse 190, CH-8057 Zurich, Switzerland.
E-mail: amedeo.caflisch@chem.uzh.ch

Author Contributions

‡These authors contributed equally.

Notes

The authors declare no competing financial interest.

ACKNOWLEDGMENT

This work was funded by SNF-Sinergia (CRSII5_180345/1) and Krebsliga (KFS-4585-08-2018) grants. The Forschungskredit from the University of Zurich is acknowledged for financial support to I.C.-S. (FK-21-114). We acknowledge the Swedish National Infrastructure for Computing (SNIC) at the High-Performance Computing Center North (HPC2N) for generously providing the computational resources. This work was supported by the International Postdoc Grant funded by the Swedish Research Council (Grant VR 2019-00608 to Y.L.). We thank Dr. Lars Wiedmer and Dr. Ivan Corbeski for support with the biochemical assays in the initial and final phase of this project, respectively. We thank Vincent Freiburghaus and Joël Bernet for the synthesis of some building blocks.

ABBREVIATIONS

PROTAC, Proteolysis Targeting Chimera; CBP, CREB-binding protein; EP300, E1A-associated protein; HAT, histone acetyltransferase; BRD, bromodomain; Ac-lysine, acetylated lysine; LE, ligand efficiency; SAR, structure-activity relationship; FluoPPI, Fluorescent based technology detecting Protein-Protein Interactions; POI, protein of interest; PPIs, protein-protein interactions; cryoEM, cryogenic electron microscopy; CRBN, Cereblon; MD, molecular dynamics; SASA, Solvent Accessible Surace Area; TR-FRET, Time-Resolved Fluorescence Energy Transfer; ZFP91, Zinc Finger Protein 91; IKZF1/3, IKAROS Family Zinc Finger 1/3; PEG, polyethylenglycol; h, hours.

REFERENCES

(1) Sakamoto, K. M.; Kim, K. B.; Kumagai, A.; Mercurio, F.; Crews, C. M.; Deshaies, R. J. Protacs: Chimeric Molecules that Target Proteins to the Skp1–Cullin–F Box Complex for Ubiquitination and Degradation. *Proc. Natl. Acad. Sci. U. S. A.* **2001**, *98*, 8554–8559.

(2) Schneekloth Jr, J. S.; Fonseca, F. N.; Koldobskiy, M.; Mandal, A.; Deshaies, R.; Sakamoto, K.; Crews, C. M. Chemical Genetic Control of Protein Levels: Selective in Vivo Targeted Degradation. *J. Am. Chem. Soc.* **2004**, *126*, 3748–3754.

(3) Lai, A. C.; Crews, C. M. Induced Protein Degradation: an Emerging Drug Discovery Paradigm. *Nat. Rev. Drug Discov.* **2017**, *16*, 101–114.

(4) Békés, M.; Langley, D. R.; Crews, C. M. PROTAC Targeted Protein Degraders: the Past is Prologue. *Nat. Rev. Drug Discov*. **2022**, *21*, 181–200.

(5) Bondeson, D. P.; Smith, B. E.; Burslem, G. M.; Buhimschi, A. D.; Hines, J.; Jaime-Figueroa, S.; Wang, J.; Hamman, B. D.; Ishchenko, A.; Crews, C. M. Lessons in PROTAC Design from Selective Degradation with a Promiscuous Warhead. *Cell Chem. Biol.* **2018**, *25*, 78–87.

(6) Smith, B. E.; Wang, S. L.; Jaime-Figueroa, S.; Harbin, A.; Wang, J.; Hamman, B. D.; Crews, C. M. Differential PROTAC Substrate Specificity Dictated by Orientation of Recruited E3 Ligase. *Nat. Commun.* **2019**, *10*, 131.

(7) Tovell, H.; Testa, A.; Zhou, H.; Shpiro, N.; Crafter, C.; Ciulli, A.; Alessi, D. R. Design and Characterization of SGK3-PROTAC1, an Isoform Specific SGK3 Kinase PROTAC Degrader. *ACS Chem. Bio*. **2019**, *14*, 2024–2034.

(8) Edmondson, S. D.; Yang, B.; Fallan, C. Proteolysis Targeting Chimeras (Protacs) in 'Beyond Rule-of-Five' Chemical Space: Recent Progress and Future Challenges. *Bioorg. Med. Chem. Lett*. **2019**, *29*, 1555−1564.

(9) Maple, H. J.; Clayden, N.; Baron, A.; Stacey, C.; Felix, R. Developing Degraders: Principles and Perspectives on Design and Chemical Space. *MedChemComm* **2019**, *10*, 1755−1764.

(10) Pye, C. R.; Hewitt, W. M.; Schwochert, J.; Haddad, T. D.; Townsend, C. E.; Etienne, L.; Lao, Y.; Limberakis, C.; Furukawa, A.; Mathiowetz, A. M.; Price, D. A.; Liras, S.; Lokey, R. S. Nonclassical Size Dependence of Permeation Defines Bounds for Passive Adsorption of Large Drug Molecules. *J. Med. Chem*. **2017**, *60*, 1665−1672.

(11) Poongavanam, V.; Atilaw, Y.; Siegel, S.; Giese, A.; Lehmann, L.; Meibom, D.; Erdelyi, M.; Kihlberg, J. Linker-Dependent Folding Rationalizes PROTAC Cell Permeability. *J. Med. Chem.* **2022**, *65*, 13029−13040.

(12) Hendrick, C. E.; Jorgensen, J. R.; Chaudhry, C.; Strambeanu, I. I.; Brazeau, J.-F.; Schiffer, J.; Shi, Z.; Venable, J. D.; Wolkenberg, S. E.; Direct-to-Biology Accelerates PROTAC Synthesis and the Evaluationof Linker Effects on Permeability and Degradation. ACS Med. Chem. Lett. 2022, 13, 1182–1190.

(13) Weerakoon, D.; Carbajo, R. J.; De Maria, L.; Tyrchan, C.; Zhao, H. Impact of PROTAC Linker Plasticity on the Solution Conformations and Dissociation of the Ternary Complex. J. Chem. Inf. Model. 2022, 62, 340–349

(14) Atilaw, Y.; Poongavanam, V.; Nilsson, C. S.; Nguyen, D.; Giese, A.; Meibom, D.; Erdelyi, M.; Kihlberg, J. Solution Conformations Shed Light on PROTAC Cell Permeability. *ACS Med. Chem. Lett.* **2021**, *12*, 107−114.

(15) Klein, V. G.; Bond, A. G.; Craigon, C.; Lokey, R. S.; Ciulli, A. Amide-to-Ester Substitution as a Strategy for Optimizing PROTAC Permeability and Cellular Activity. *J. Med. Chem*. **2021**, *64*, 18082–18101.

(16) Shaha, R. R.; Redmonda, J. M.; Mihuta, A.; Menona, M.; Evansa, J. P.; Murphy, J. A.; Bartholomewa, M. A.; Coea, D. M. Hi-JAK-ing the Ubiquitin System: The Design and Physicochemical Optimisation of JAK PROTACs. *Bioorg. Med. Chem*. **2020**, *28*, 115326.

(17) Klein, V. G.; Townsend, C. E.; Testa, A.; Zengerle, M.; Maniaci, C.; Hughes, S. J.; Chan, K.-H.; Ciulli, A.; Lokey, R. S. Understanding and Improving the Membrane Permeability of VH032-Based PROTACs. *ACS Med. Chem. Lett*. **2020**, *11*, 1732−1738.

(18) Zhu, K.-F.; Yuan, C.; Du, Y.-M.; Sun, K.-L.; Zhang, X.-K.; Vogel, H.; Jia, X.-D.; Gao, Y.-Z.; Zhang, Q.-F.; Wang, D.-P.; Zhang, H.-W. Applications and Prospects of Cryo-EM in Drug Discovery. *Military Med. Res.* **2023**, *10*, 27.

(19) Kofink, C.; Trainor,N.; Mair, B.; Wöhrle, S.; Wurm, M.; Mischerikow, N.; Roy, M. J.; Bader, G.; Greb, P.; Garavel, G.; Diers, E.; McLennan, R.; Whitworth, C.; Vetma, V.; Rumpel, K.; Scharnweber, M.; Fuchs, J. E.; Gerstberger, T.; Cui, Y.; Gremel, G.; Chetta, P.; Hopf, S.; Budano, N.; Rinnenthal, J.; Gmaschitz, G.; Mayer, M.; Koegl, M.; Ciulli, A.; Weinstabl, H.; Farnaby, W. A Selective and Orally Bioavailable VHL-recruiting PROTAC Achieves SMARCA2 Degradation in Vivo. *Nat. Commun*. **2022**, *13*, 5969.

(20) Testa, A.; Hughes, S. J.; Lucas, X.; Wright, J. E.; Ciulli, A. Structure-Based Design of a Macrocyclic PROTAC. *Angew. Chem. Int. Ed.* **2020**, *59*, 1727–1734.

(21) Farnaby, W.; Koegl, M.; Roy, M. J.; Whitworth, C.; Diers, E.; Trainor, N.; Zollman, D.; Steurer, S.; Karolyi-Oezguer, J.; Riedmueller, C.; Gmaschitz, T.; Wachter, J.; Dank, C.; Galant, M.; Sharps, B.; Rumpel, K.; Traxler, E.; Gerstberger, T.; Schnitzer, R.; Petermann, O.; Greb, P.; Weinstabl, H.; Bader, G.; Zoephel, A.; Weiss-Puxbaum, A.; Ehrenhöfer-Wölfer, K.; Wöhrle, S.; Boehmelt, G.; Rinnenthal, J.; Arnhof, H.; Wiechens, N.; Wu, M.-Y.; Owen-Hughes, T.; Ettmayer, P.; Pearson, M.; McConnell, D. B.; Ciulli, A. BAF Complex Vulnerabilities in Cancer Demonstrated via Structure-based PROTAC Design. *Nat. Chem. Biol*. **2019**, *15*, 672–680.

(22) Hughes, S. J.; Ciulli, A. Molecular Recognition of Ternary Complexes: a New Dimension in the Structure-Guided Design of Chemical Degraders. *Essays Biochem*. **2017**, *61*, 505−516.

(23) Gadd, M. S.; Testa, A.; Lucas, X.; Chan, K.-H. Chen, W.; Lamont, D. J.; Zengerle, M.; Ciulli, A. Structural Basis of PROTAC Cooperative Recognition for Selective Protein Degradation. *Nat. Chem. Biol*. **2017**, *13*, 514–521.

(24) Heintzman, N. D.; Stuart, R. K.; Hon, G.; Fu, Y.; Ching, C. W.; Hawkins, R. D.; Barrera, L. O.; van Calcar, S.; Qu, C.; Ching, K. A.; Wang, W.; Weng, Z.; Green, R. D.; Crawford, G. E.; Ren, B. Distinct and Predictive Chromatin Signatures of Transcriptional Promoters and Enhancers in the Human Genome. *Nat. Gen.* **2007**, *39*, 311–318.

(25) Visel, A.; Blow, M. J.; Li, Z.; Zhang, T.; Akiyama, J. A.; Holt, A.; Plajzer-Frick, I.; Shoukry, M.; Wright, C.; Chen, F.; Afzal, V.; Ren, B; Rubin, E. M.; Pennacchio, L. A. ChIP-seq Accurately Predicts Tissue-Specific Activity of Enhancers. *Nature* **2009**, *457*, 854–858.

(26) Xi, H.; Shulha, H. P.; Lin, J. M.; Vales, T. R.; Fu, Y.; Bodine, D. M.; McKay, R. D. G.; Chenoweth, J. G.; Tesar, P. J.; Furey, T. S.; Ren, B.; Weng, Z.; Crawford, G. E. Identification and Characterization of Cell Type–Specific and Ubiquitous Chromatin Regulatory Structures in the Human Genome. *PLoS Genet*. **2007**, *3*, 1377.

(27) Dancy, B. M.; Cole, P. A. Protein Lysine Acetylation by p300/CBP. *Chem. Rev*. **2015**, *115*, 2419–2452.

(28) Weinert, B. T.; Narita, T.; Satpathy, S.; Srinivasan, B.; Hansen, B. K.; Schölz, C.; Hamilton, W. B.; Zucconi, B. E.; Wang, W. W.; Liu, W. R.; Brickman, J. M.; Kesicki, E. A.; Lai, A.; Bromberg, K. D.; Cole, P. A.; Choudhary, C. Time-Resolved Analysis Reveals Rapid Dynamics and Broad Scope of the CBP/p300 Acetylome. *Cell* **2018**, *174*, 231–244.

(29) Ogryzko, V. V.; Schiltz, R. L.; Russanova, V.; Howard, B. H.; Nakatani, Y. The Transcriptional Coactivators p300 and CBP are Histone Acetyltransferases. *Cell* **1996**, *87*, 953–959.

(30) van Gils, J.; Magdinier, F.; Fergelot, P.; Lacombe, D.; Rubinstein-Taybi Syndrome: A Model of Epigenetic Disorder. *Genes* **2021**, *12*, 968.

(31) Attar, N.; Kurdistani, S. K.; Exploitation of EP300 and CREBBP Lysine Acetyltransferases by Cancer. *Cold Spring Harbor Perspect. Med.* **2017**, *7*, a026534.

(32) Farria, A.; Li, W.; Dent, S. Y. R. KATs in Cancer: Functions and Therapies. *Oncogene* **2015**, *34*, 4901–4913.

(33) Valor, L. M.; Viosca, J.; Lopez-Atalaya, J. P.; Barco, A. Lysine Acetyltransferases CBP and p300 as Therapeutic Targets in Cognitive and Neurodegenerative Disorders. *Curr. Pharm. Des.* **2013**, *19*, 5051–5064.

(34) Ghizzoni, M.; Haisma, H. J.; Maarsingh, H.; Dekker, F. J. Histone Acetyltransferases are Crucial Regulators in NF-κB Mediated Inflammation. *Drug Discov. Today* **2011**, *16*, 504-511.

(35) Romero, F. A.; Murray, J.; Lai, K. W.; Tsui, V.; Albrecht, B. K.; An, L.; Beresini, M. H.; de Leon Boenig, G.; Bronner, S. M.; Chan, E. W.; Chen, K. X.; Chen, Z.; Choo, E. F.; Clagg, K.; Clark, K.; Crawford, T. D.; Cyr, P.; de Almeida Nagata, D.; Gascoigne, K. E.; Grogan, J. L.; Hatzivassiliou, G.; Huang, W.; Hunsaker, T. L.; Kaufman, S.; Koenig, S. G.; Li, R.; Li, Y.; Liang, X.; Liao, J.; Liu, W.; Ly, J.; Maher, J.; Masui, C.; Merchant, M.; Ran, Y.; Taylor, A. M.; Wai, J.; Wang, F.; Wei, X.; Yu, D.; Zhu, B.-Y.; Zhu, X.; Magnuson, S. GNE-781, A Highly Advanced Potent and Selective Bromodomain Inhibitor of Cyclic Adenosine Monophosphate Response Element Binding Protein, Binding Protein (CBP). *J. Med. Chem.* **2017**, *60*, 9162–9183.

(36) Lai, K. W.; Romero, F. A.; Tsui, V.; Beresini, M. H.; de Leon Boenig, G.; Bronner, S. M.; Chen, K.; Chen, Z.; Choo, E. F.; Crawford, T. D.; Cyr, P.; Kaufman, S.; Li, Y.; Liao, J.; Liu, W.; Ly, J.; Murray, J.; Shen, W.; Wai, J.; Wang, F.; Zhu, C.; Zhu, X.; Magnuson, S. Design and Synthesis of a Biaryl Series as Inhibitors for the Bromodomains of CBP/P300. *Bioorganic Med. Chem. Lett*. **2018**, *28*, 15–23.

(37) Welti, J.; Sharp, A.; Brooks, N.; Yuan, W.; McNair, C.; N. Chand, S.; Pal, A.; Figueiredo, I.; Riisnaes, R.; Gurel, B.; Rekowski, J.; Bogdan, D.; West, W.; Young, B.; Raja, M.; Prosser, A.; Lane, J.; Thomson, S.; Worthington, J.; Onions, S.; Shannon, J.; Paoletta, S.; Brown, R.; Smyth, D.; Harbottle, G. W.; Gil, V. S.; Miranda, S.; Crespo, M.; Ferreira, A.; Pereira, R.; Tunariu, N.; Carreira, S.; Neeb, A. J.; Ning, J.; Swain, A.; Taddei, D.; Schiewer, M. J.; Knudsen, K. E.; Pegg, N.; de Bono, J. S. Targeting the p300/CBP Axis in Lethal Prostate Cancer. *Cancer Discov*. **2021**, *11*, 1118–1137.

(38) Lasko, L. M.; Jakob, C. G.; Edalji, R. P.; Qiu, W.; Montgomery, D.; Digiammarino, E. L.; Hansen, T. M.; Risi, R. M.; Frey, R.; Manaves, V.; Shaw, B.; Algire, M.; Hessler, P. Lam, L. T.; Uziel, T.;

Faivre, E.; Ferguson, D.; Buchanan, F. G.; Martin, R. L.; Torrent, M.; Chiang, G. G.; Karukurichi, K.; William Langston, J., Weinert, B. T.; Choudhary, C.; de Vries, P.; Kluge, A. F.; Patane, M. A.; Van Drie, J. H.; Wang, C.; McElligott, D.; Kesicki, E. A.; Marmorstein, R.; Sun, C.; Cole, P.A.; Rosenberg, S. H.; Michaelides, M. R.; Lai, A.; Bromberg, K. D. Discovery of a Selective Catalytic p300/CBP Inhibitor that Targets Lineage-Specific Tumours. *Nature* **2017**, *550*, 128–132.

(39) Wilson, J. E.; Patel, G.; Patel, C.; Brucelle, F.; Huhn, A.; Gardberg, A. S.; Poy, F.; Cantone, N.; Bommi-Reddy, A.; Sims, R. J.; Cummings, R. T.; Levell, J. R. Discovery of CPI-1612: A Potent, Selective, and Orally Bioavailable EP300/CBP Histone Acetyltransferase Inhibitor. *ACS Med. Chem. Lett*. **2020**, *11*, 1324–1329.

(40) Cheng-Sánchez, I.; Gosselé, K. A.; Palaferri, L.; Kirillova, M. S.; Nevado, C. Discovery and Characterization of Active CBP/EP300 Degraders Targeting the HAT Domain. *ACS Med. Chem. Lett*. **2023**. Article ASAP. DOI: 10.1021/acsmedchemlett.3c00490.

(41) Vannam, R.; Sayilgan, J.; Ojeda, S.; Karakyriakou, B.; Hu, E.; Kreuzer, J.; Morris, R.; Lopez, X. I. H.; Rai, S.; Haas, W.; Lawrence, M.; Ott, C. J. Targeted Degradation of the Enhancer Lysine Acetyltransferases CBP and p300. *Cell Chem. Bio*. **2021**, *28*, 503–514.

(42) Durbin, A. D.; Wang, T.; Wimalasena, V. K.; Zimmerman, M. W.; Li, D.; Dharia, N. V.; Mariani, L.; Shendy, N. A. M.; Nance, S.; Patel, A. G.; Shao, Y.; Mundada, M.; Maxham, L.; Park, P. M.C.; Sigua, L. H.; Morita, K.; Conway, A. S.; Robichaud, A. L.; Perez-Atayde, A. R.; Bikowitz, M. J.; Quinn, T. R.; Wiest, O.; Easton, J.; Schönbrunn, E.; Bulyk, M. L.; Abraham, B. J.; Stegmaier, K.; Thomas Look, A.; Qi, J. EP300 Selectively Controls the Enhancer Landscape of MYCN-Amplified Neuroblastoma. *Cancer Discov*. **2022**, *12*, 730–751.

(43) Thomas II, J. E.; Wang, M.; Jiang, W.; Wang, M.; Wang, L.; Wen, B.; Sun, D.; Wang, S. Discovery of Exceptionally Potent, Selective, and Efficacious PROTAC Degraders of CBP and p300 Proteins. *J. Med. Chem.* **2023**, *66*, 8178–8199.

(44) Chang, Q.; Li J.; Deng Y.; Zhou R.; Wang B.; Wang Y.; Zhang M.; Huang X.; Li Y. Discovery of Novel PROTAC Degraders of p300/CBP as Potential Therapeutics for Hepatocellular Carcinoma. *J. Med. Chem.* **2024**, Article ASAP. DOI: 10.1021/acs.jmedchem.3c01468.

(45) Batiste, L.; Unzue, A.; Dolbois, A.; Hassler, F.; Wang, X.; Deerain, N.; Zhu, J.; Spiliotopoulos, D.; Nevado, C.; Caflisch, A. Chemical Space Expansion of Bromodomain Ligands Guided by in Silico Virtual Couplings (AutoCouple). *ACS Cent. Sci.* **2018**, *4*, 180–188.

(46) Manuscript in preparation.

(47) Majeux, N.; Scarsi, M.; Apostolakis, J.; Ehrhardt, C.; Caflisch, A. Exhaustive Docking of Molecular Fragments with Electrostatic Solvation. *Proteins: Structure, Function, and Bioinformatics* **1999**, *37*, 88–105.

(48) Huang, D.; Lüthi, U.; Kolb, P.; Cecchini, M.; Barberis, A.; Caflisch, A. In Silico Discovery of β-Secretase Inhibitors. *J. Am. Chem. Soc*. **2006**, 128, 5436–5443.

(49) Friedman, R.; Caflisch A. Discovery of Plasmepsin Inhibitors by Fragment-Based Docking and Consensus Scoring. *ChemMedChem* **2009**, *4*, 1317–1326.

(50) Xu, M.; Unzue, A.; Dong, J.; Spiliotopoulos, D.; Nevado, C.; Caflisch, A. Discovery of CREBBP Bromodomain Inhibitors by High-Throughput Docking and Hit Optimization Guided by Molecular Dynamics. *J. Med. Chem*. **2016**, *59*, 1340–1349.

(51) Ekonomiuk, D.; Su, X.-C.; Ozawa, K.; Bodenreider, C.; Lim, S. P.; Yin, Z.; Keller, T. H.; Beer, D.; Patel, V.; Otting, G.; Caflisch, A.; Huang, D. Discovery of a Non-Peptidic Inhibitor of West Nile Virus NS3 Protease by High-Throughput Docking. *PLOS Neglected Tropical Diseases* 2009, 3(1): e356.

(52) Marchand, J.-R.; Vedove, A. D.; Lolli, G.; Caflisch, A. Discovery of Inhibitors of Four Bromodomains by Fragment-Anchored Ligand Docking. *J. Chem. Inf. Model*. **2017**, *57*, 2584–2597.

(53) Ekonomiuk, D.; Su, X.-C.; Ozawa, K.; Bodenreider, C.; Lim, S. P.; Otting, G.; Huang, D.; Caflisch, A. Flaviviral Protease Inhibitors Identified by Fragment-Based Library Docking into a Structure Generated by Molecular Dynamics. *J. Med. Chem.* **2009**, *52*, 4860–4868.

(54) Marchand, J.-R.; Caflisch, A. In silico fragment-based drug design with SEED. *Eur. J. Med. Chem*. **2018**, *156*, 907–917.

(55) . Goossens, K.; Wroblowski, B.; Langini, C.; van Vlijmen, H.; Caflisch, A. Assessment of the Fragment Docking Program SEED. *J. Chem. Inf. Model* 2020, *60*, 4881–4893.

(56) Vanommeslaeghe, K.; Hatcher, E.; Acharya, C.; Kundu, S.; Zhong, S.; Shim, J.; Darian, E.; Guvench, O.; Lopes, P.; Vorobyov, I.; Mackerell Jr., A. D. CHARMM General Force Field: A Force Field for Drug-Like Molecules Compatible with The CHARMM All-Atom Additive Biological Force Fields. *J. Comput. Chem*. 2010, *31*, 671–690.

(57) Scarsi, M.; Apostolakis, J.; Caflisch, A. Continuum Electrostatic Energies of Macromolecules in Aqueous Solutions. *J. Phys. Chem. A* 1997, *101*, 8098–8106.

(58) Vanommeslaeghe, K.; MacKerell, A. D. Jr. Automation of the CHARMM General Force Field (CGenFF) I: Bond Perception and Atom Typing. *J. Chem. Inf. Model*. **2012**, *52*, 3144–3154.

(59) Ghayor, C.; Gjoksi, B.; Dong, J.; Siegenthaler, B.; Caflisch, A.; Weber, F. E. N, N Dimethylacetamide a Drug Excipient that Acts as Bromodomain Ligand for Osteoporosis Treatment. *Sci. Rep.* 2017, *7*, 1–10.

(60) Spiliotopoulos, D.; Zhu, J.; Wamhoff, E.-C.; Deerain, N.; Marchand, J.-R.; Aretz, J.; Rademacher, C.; Caflisch, A. Virtual Screen to NMR (VS2NMR): Discovery of Fragment Hits for the CBP Bromodomain. *Bioorg. Med. Chem. Lett.* **2017**, *27*, 2472–2478.

(61) For the extended PROTAC screening see Supporting Information.

(62) An, J.; Ponthier, C. M.; Sack, R.; Seebacher, J.; Stadler, M. B.; Donovan, K. A.; Fischer, E. S. pSILAC Mass Spectrometry Reveals ZFP91 as IMiD-Dependent Substrate of the CRL4CRBN Ubiquitin Ligase. *Nat. Commun.* **2017**, *8*, 15398.

(63) Watanabe, T.; Seki, T.; Fukano, T.; Sakaue-Sawano, A.; Karasawa, S.; Kubota, M.; Kurokawa, H.; Inoue, K.; Akatsuka, J.; Miyawaki, A. Genetic Visualization of Protein Interactions Harnessing Liquid Phase Transitions. *Sci. Rep*. **2017**, *7*, 46380.

(64) Doak, B. C.; Over, B.; Giordanetto, F.; Kihlberg, J. Oral Druggable Space beyond the Rule of 5: Insights from Drugs and Clinical Candidates. *Chem. Biol*. **2014**, *21*, 1115−1142.

.Insert Table of Contents artwork here